Octahedral tilting in strained $LaVO_3$ thin films

H. Rotella,[1,*] U. Lüders,[1] P.-E. Janolin,[2] V. H. Dao,[1] D. Chateigner,[1] R. Feyerherm,[3] E. Dudzik,[3] and W. Prellier[1,†]

[1]*Laboratoire CRISMAT, Normandie Université, ENSICAEN, CNRS UMR 6508, 6 Boulevard Maréchal Juin, 14050 Caen Cedex 4, France*

[2]*Laboratoire Structures, Propriétés et Modélisation des Solides, UMR CNRS-École Centrale Paris, Grande Voie des Vignes, 92295 Châtenay-Malabry Cedex, France*

[3]*Helmholtz-Zentrum Berlin für Materialien und Energie GmbH, BESSY, Albert-Einstein-Strasse 15, 12489 Berlin, Germany*

(Received 5 April 2012; published 11 May 2012)

The effect of biaxial strain on the oxygen octahedra rotations in a $LaVO_3$ thin film is investigated using synchrotron radiation. First, we find that the film adopts a distorted orthorhombic structure under the compressive stress induced by the $SrTiO_3$ substrate. Second, we separate the contribution to the superstructure peaks arising from cation displacement and VO_6 rotations in order to quantify the rotation angles. Finally, we find an original $a^-a^+c^-$ tilt system, which is induced by the biaxial strain imposed by the substrate. These quantitative results may open up new directions for understanding the modification of electronic properties of engineered oxide films.

DOI: 10.1103/PhysRevB.85.184101 PACS number(s): 81.15.Fg, 68.55.A−, 61.05.cp

I. INTRODUCTION

The ABO_3 perovskite oxide compounds constitute a very attractive class of materials because of the broad spectra of functional properties they exhibit, such as metal-insulator transition, ferroelectricity, superconductivity, etc.[1–5] It is well known that these properties are strongly related to the structure of such materials, and it has been shown that structure distortions are critical.[6–8] The origin of this coupling results from the important role of the cation-anion bond length and angle. Also, in the physics of perovskite oxides, highly directional d orbitals with quite localized charge carriers are typically involved.[9] The majority of the perovskite group compounds are distorted derivatives of the parent cubic [$Pm\bar{3}m$ (no. 221)] resulting from a combination of the following contributions: (i) tilting of BO_6 octahedra; (ii) first-order Jahn-Teller distortion of BO_6 octahedra; (iii) second-order Jahn-Teller effects on A and B displacement; and (iv) cation displacement, even if the main mechanism is the tilt of the octahedra for most of the perovskite oxides.

Several external parameters, such as temperature, pressure, stress, etc., may also cause these distortions. More specifically, for tilts of BO_6 octahedra, increasing temperature generally leads to a reduction of the tilt angle whereas high hydrostatic pressure may lead either to an increase of the tilt angle (e.g., among numerous examples,[10,11] which was long considered to be the only possibility[12]) or to a decrease.[13–17] In the case of $CaTiO_3$, it may also leave the tilt angle unchanged.[18] The main feature of a recent model[16,17] is that $A^{2+}B^{4+}O_3$ perovskites should have their tilt angles increase under hydrostatic pressure whereas they should decrease for $A^{3+}B^{3+}O_3$. However, the influence of biaxial strain on the tilt angles, as in the case of thin films, has not been tackled systematically yet.

The standard description for octahedral rotations in perovskite compounds, first introduced by Glazer,[19] is to consider the ideal cubic structure with the position of the A cation at $(\frac{1}{2}\frac{1}{2}\frac{1}{2})$. The position of the octahedron center is at the corner of the unit cell and its rotation is a combination of rotations around each cubic axis $[100]_p$, $[010]_p$, and $[001]_p$. The magnitude of the rotation angle is denoted by a, b, or c. Using the same letter for two directions indicates that the magnitudes of the angles are the same around both directions. The sense of the rotation in successive layers of octahedra along the rotation axis is given by a superscript + or −, which denotes in-phase or antiphase tilts, respectively. Since the tilt system is also directly correlated to the structure symmetry, Glazer, followed by Woodward, have associated each tilt system to a space group based on crystallographic principles.[20–22]

The strong interplay between lattice distortions, octahedral tilts, and physical properties of functional perovskite oxides can be used either to study the influence of distortions on the properties, or to tune the properties by distorting the lattice in a controlled way. In the case of epitaxial thin films, the strain, and therefore the lattice distortions, are mainly controlled by the difference of the lattice parameters between the substrate material and the bulk "related" ones. The usefulness of this method to create new properties in perovskite oxides has been shown recently by the emergence of ferroelectricity in $CaMnO_3$ strained films.[23–25] However, the exact structure of distorted perovskite thin films is difficult to characterize because of the reduced volume and the single crystalline character with a peculiar orientation of thin films. Recently, the structure of strained $LaNiO_3$ thin film was successfully analyzed.[26] This was only possible because this compound adopts a rhombohedral structure and an (a^- a^- a^-) tilt system in Glazer's notation[19,21,22] which excludes any distortion mechanism other than octahedral rotations.[22] In more complex systems, the distortions of the lattice are usually used to infer the change in the tilt system,[27] but the quantitative information is lost. However, the value of rotation angles is required to evaluate the cation-anion bond distortions and thus explain emergent properties in perovskite oxide thin films.

For this reason, we have conducted an in-depth structural analysis of $LaVO_3$ thin films. $LaVO_3$ has the $GdFeO_3$ structure and is thus isostructural to a large number of functional perovskites. More precisely, it adopts a $Pnma$ (no. 62) orthorhombic structure at room temperature,[28] which has the ($a^-b^+a^-$) tilting system, corresponding to many structure among the RMO_3 families, where R denotes rare earth and M denotes transition metal.[29,30] Perovskites with $Pnma$ structure are well known to present both octahedral rotation and cation displacement.[22] The investigation of rare-earth

orthovanadates, RVO_3, is very interesting due to various properties including spin and orbital orders which are strongly dependent on the crystal symmetry.[31,32] Furthermore, the low mismatch between pseudocubic $LaVO_3$ and $SrTiO_3$ substrate lattice parameters (0.5% at room temperature) and thermal expansion coefficients results in rather thick, high-quality, and coherently strained thin films, which are ideal to achieve a high experimental accuracy on the structure of the film.

Apart from these methodological advantages, $LaVO_3$ was shown to change from its antiferromagnetic, insulating properties in bulk to a magnetic, highly conducting phase in superlattices with $SrVO_3$.[33,34] $LaVO_3$ being a Mott insulator,[35] structural distortions under compressive strain may have dramatic consequences on its properties. In order to elucidate the exact origin of this modification of the properties, determining the change of the V-O bonds in the strained $LaVO_3$ is crucial. Our structural analysis of $LaVO_3$ will allow us to evaluate qualitatively the different distortion mechanisms present in the thin film and quantitatively the rotation angles of the tilt system.

II. EXPERIMENTS

Epitaxial $LaVO_3$ (LVO) thin film was prepared by the pulsed laser deposition technique on a (001)-oriented $SrTiO_3$ (STO) substrate (cubic $a = 3.905$ Å).[36] In the following study, the subscripts o and p refer to the orthorhombic and pseudocubic descriptions of the system, respectively. In bulk form, the lattice parameters of LVO are, at room temperature, $a_o = 5.5529(2)$ Å, $b_o = 7.8447(3)$ Å, and $c_o = 5.5529(3)$ Å.[28] When considering the pseudocubic subcell, the lattice parameters become $a_p \simeq a_o/\sqrt{2} \simeq b_o/2 \simeq c_o/\sqrt{2} \simeq 3.9251(1)$ Å. The mismatch between $a_{p_{LVO}}$ and a_{STO} is about 0.5%, indicating a compressive stress. A KrF laser ($\lambda = 248$ nm) with a repetition rate of 3 Hz and a fluence of $\simeq 2$ J/cm^2 was focused onto a $LaVO_4$ polycrystalline target. The substrate is kept at 700 °C under a dynamic vacuum around 10^{-5} mbar. The distance between the target and the substrate is 8.5 cm. Those conditions were chosen according to previous studies.[37,38] Preliminary x-ray diffraction (XRD) measurements were done in Caen, France with a Seifert diffractometer Cu $K\alpha_1$ ($\lambda = 1.5406$ Å) to verify the quality of the samples. All other measurements have been carried out at room temperature using the four circle diffractometer at beamline 7T-MPW-MAGS at the synchrotron source BESSY II at Helmholtz-Zentrum, Berlin. The photon energy 12.398 keV was chosen ($\lambda = 1$ Å).

III. RESULTS

The XRD pattern of a 730-Å film is presented in Fig. 1. The graph indicates that the film is oriented along the $(002)_p$ direction of the cubic subcell. The high quality is shown by the presence of Laue fringes. The pseudocubic out-of-plane lattice parameter was calculated to be equal to 3.945(1) Å, in agreement with a film grown under in-plane compressive stress. The thickness of the film is further confirmed by the simulation of the Laue reflections, close to 734 Å, i.e., 186 pseudocubic cells. Further investigations were performed using synchrotron radiation at BESSY II. The azimuthal ϕ scans recorded, for the film and the substrate, along the

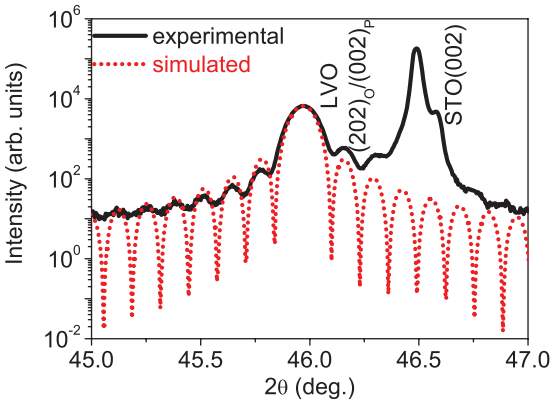

FIG. 1. (Color online) θ-2θ XRD pattern of $LaVO_3$ film grown on a (001)-oriented $SrTiO_3$ substrate, recorded along the [002] direction of $SrTiO_3$. The presence of the Laue fringes around the (202) diffraction peak of the $LaVO_3$ film attests to the high quality of the sample, both in terms of surface and interface roughness. The simulation of the spectra was done with DIFFAX taking into account only the film contribution.[40] The matching between the experimental spectra and the simulation confirms the thickness of the film closed to 734 Å, corresponding to 186 pseudocubic unit cells.

$(103)_p$ reflection (Fig. 2) indicate the cube-on-cube epitaxial growth with the relations $[001]_F \parallel [001]_S$ and $[100]_F \parallel [100]_S$, considering a cubic description for the film. The position of the $(103)_p$ reflection shows a pseudocubic in-plane lattice parameter of 3.91(3) Å equal to the substrate. Previous studies made on $LaVO_3/SrVO_3$ superlattices have emphasized that epitaxial relations between LVO and STO, taking into account the orthorhombic description, are $[101]_F \parallel [001]_S$ and $[010]_F \parallel [100]_S$ or $[010]_F \parallel [010]_S$, which allows for the presence of structural domains at 90° in the film.[39]

Experimentally, considering the orthorhombic structure of $LaVO_3$, the asymmetric peaks $(204)_o$, $(402)_o$, $(323)_o$, and $(3\text{-}23)_o$, corresponding to the family of the $\{103\}_p$ reflections (see Fig. 3), were measured and we do not observe any splitting. This means that the in-plane pseudocubic lattice

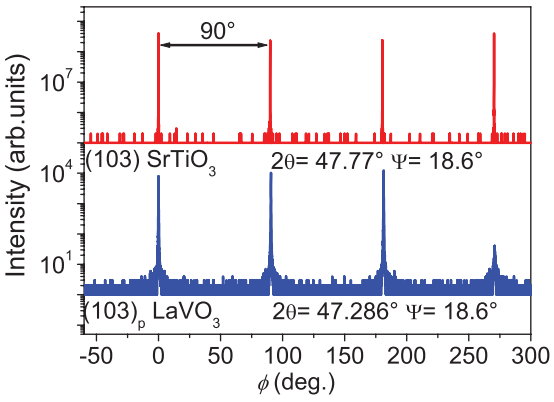

FIG. 2. (Color online) XRD ϕ scans recorded along the (103) direction of the (001)-oriented $SrTiO_3$ substrate (bottom panel) and the $(103)_p$ pseudocubic direction of the $LaVO_3$ film (top panel). The alignment of both scans confirms a cube-on-cube epitaxy of $LaVO_3$ thin film grown on a (001)-oriented $SrTiO_3$ substrate, considering a pseudocubic description for $LaVO_3$ (see text for details).

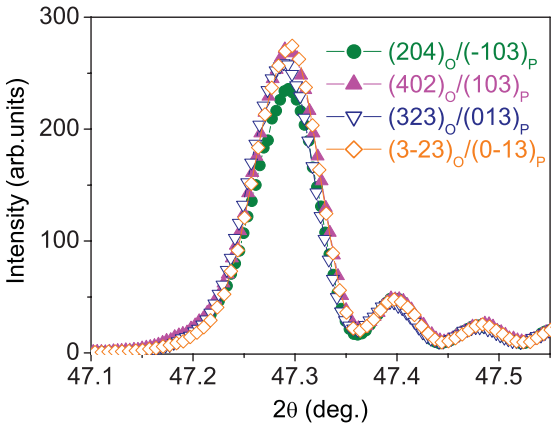

FIG. 3. (Color online) $LaVO_3$ XRD patterns recorded around the asymmetric diffraction peaks $(204)_o$, $(402)_o$, $(323)_o$, and $(3\text{-}23)_o$ corresponding to the 103_p family. The matching between the intensities and the positions of the four peaks indicates that c_p is normal to the substrate plane.

parameters are equal ($a_p = b_p$), which leads to the relation $b_o = 2a_p$. Considering only these reflections, we were not able to observe the 90°-oriented domains noticed in a previous study.[39] The four reflections are at the same 2θ value within resolution limit, indicating that the out-of-plane cubic parameter of the film is orthogonal to the plane of the substrate. This observation suggests two descriptions for the film. The first one is a tetragonal symmetry with $a_p = b_p = 3.91(3)$ Å, $c_p = 3.945(1)$ Å, whereas the second corresponds to the actual symmetry adopted by LVO due to the presence of octahedral rotation, i.e., a distorted orthorhombic description with $a_o = c_o = 5.55(2)$ Å, $b_o = 7.82(6)$ Å, $\alpha_o = \gamma_o = 90°$, and $\beta_o = 89.489(6)°$ (a schematic representation of these descriptions is shown in Fig. 4). The relaxation in the film thickness explains the difference between the measured film lattice parameter a_p and the substrate one. At this point of the study, only a distorted $Pnma$ (no. 62) or a $P2_1/m$ (no. 11) space group is compatible with the strained epitaxial $LaVO_3$ thin film, which is in agreement with previous studies made on strained orthorhombic compounds.[27]

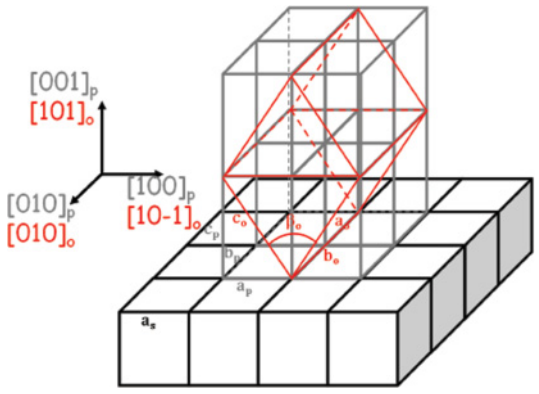

FIG. 4. (Color online) Schematic representation of the orientation of an epitaxial $LaVO_3$ thin film grown under compressive stress on a cubic (001)-oriented $SrTiO_3$ substrate. a_s is the substrate lattice parameter (3.905 Å); a_p, b_p, and c_p are the pseudocubic axes [$a_p = b_p = 3.91(3)$ Å, $c_p = 3.945(1)$ Å] and a_o, b_o, and c_o are the orthorhombic axes; and β_o is the angle between a_o and c_o [$a_o = c_o = 5.55(2)$ Å, $b_o = 7.82(6)$ Å, and $\beta_o = 89.489(6)°$].

We estimate the pseudocubic in-plane lattice parameters of $LaVO_3$ strained thin film as $a_p = b_p = 3.91(3)$ Å. By comparing the bulk pseudocubic lattice parameter, we evaluate the residual stress value induced by the substrate. The generalized form of Hooke's law is written as

$$\sigma_i = c_{ij}\epsilon_j, \tag{1}$$

where σ_i is the stress, c_{ij} is the stiffness, and ϵ_j is the strain tensors. According to Khan *et al.*,[41] the stiffness coefficients of $LaVO_3$ are

$$\begin{pmatrix} 391.3 & 158.1 & 142.7 \\ 158.1 & 399.3 & 158.1 \\ 142.7 & 158.1 & 436.5 \end{pmatrix}. \tag{2}$$

Taking into account a crystalline orientation corresponding to a rotation by 45° around the b axis,

$$\begin{pmatrix} \cos 45 & 0 & \sin 45 \\ 0 & 1 & 0 \\ -\sin 45 & 0 & \cos 45 \end{pmatrix}. \tag{3}$$

Thus, Eq. (1) leads to the following relationships (in Voigt notation):

$$\sigma_1 = \frac{(c_{11}+c_{13})}{\sqrt{2}}\epsilon_1 + \frac{(c_{12}+c_{23})}{\sqrt{2}}\epsilon_2 + \frac{(c_{13}+c_{33})}{\sqrt{2}}\epsilon_3, \tag{4}$$

$$\sigma_3 = \frac{(-c_{11}+c_{13})}{\sqrt{2}}\epsilon_1 + \frac{(-c_{12}+c_{23})}{\sqrt{2}}\epsilon_2 + \frac{(-c_{13}+c_{33})}{\sqrt{2}}\epsilon_3. \tag{5}$$

Furthermore, we know that $\epsilon_1 = \epsilon_2 = -3.847(8) \times 10^{-3}$ and $\sigma_3 = 0$. Thus, the residual biaxial stress induced by the substrate on the $LaVO_3$ thin film is $\sigma_{11} = -3.6(1)$ GPa. This value is compatible with the compressive stress already underlined in our system and in the same order of magnitude of stress found in a similar study done on epitaxial thin film.[42]

To complete the structural study on the film, the octahedral rotations have been estimated. Considering a pseudocubic description, the octahedral rotations produce half-order Bragg peaks, corresponding to forbidden reflections in the space group $Pm\bar{3}m$ (no. 221), with the system having to adopt a lower symmetry.[19] To identify the tilt system of our film, the most accessible half-order Bragg peaks were investigated. (The number of measured peaks was limited by the experimental setup of the four-circle diffractometer.) Considering pseudocubic indexing, we observed every half-order peak with the special conditions on h, k, l (all integer): (i) when h is even, k and l are odd and different, which corresponds to the reflections along the $[0\frac{k}{2}\frac{l}{2}]_p$ directions; (ii) when k is even, h and l are odd and different, associated with the reflections along the $[\frac{h}{2}0\frac{l}{2}]_p$ directions; (iii) when l is even, h and k are odd and different, associated with the reflections along the $[\frac{h}{2}\frac{k}{2}0]_p$ directions (Fig. 5); and finally (iv) when h, k, and l are all odd, $l = h$ or k, corresponding to the reflections along the directions $[\frac{h}{2}\frac{h}{2}\frac{l}{2}]_p$, $[\frac{h}{2}\frac{k}{2}\frac{h}{2}]_p$, and $[\frac{h}{2}\frac{k}{2}\frac{k}{2}]_p$. Note that the intensities of those reflections are mainly produced by the lanthanum displacement in the structure (see Table I) and have not been used to determined the tilt system.

TABLE I. Associated peaks in the diffraction pattern of $LaVO_3$ to the structure with (1) neither displacement nor octahedral rotation, (2) La displacements but no octahedral rotation, (3) octahedral rotations without La displacement, and (4) octahedral rotation and La displacement.

	Diffraction pattern			
2θ (deg)	(1) $(hkl)_o/(hkl)_p$	(2) $(hkl)_o/(hkl)_p$	(3) $(hkl)_o/(hkl)_p$	(4) $(hkl)_o/(hkl)_p$
12.61		$(110)/(\frac{1}{2}\frac{1}{2}\frac{1}{2})$		$(110)/(\frac{1}{2}\frac{1}{2}\frac{1}{2})$
14.62	(101)/(001)	(101)/(001)	(101)/(001)	(101)/(001)
16.31		$(111)/(0\frac{1}{2}1)$		$(111)/(0\frac{1}{2}1)$
20.70	(200)/(101)	(200)/(101)	(200)/(101)	(200)/(101)
22.02		$(210)/(1\frac{1}{2}1)$		$(210)/(1\frac{1}{2}1)$
23.21			$(201)/(\frac{1}{2}0\frac{3}{2})$	$(201)/(\frac{1}{2}0\frac{3}{2})$
24.36		$(211)/(\frac{1}{2}\frac{1}{2}\frac{3}{2})$	$(211)/(\frac{1}{2}\frac{1}{2}\frac{3}{2})$	$(211)/(\frac{1}{2}\frac{1}{2}\frac{3}{2})$
25.51	(220)/(111)	(220)/(111)	(220)/(111)	(220)/(111)
26.58		$(131)/(0\frac{3}{2}1)$		$(131)/(0\frac{3}{2}1)$
27.57			$(221)/(\frac{1}{2}1\frac{3}{2})$	$(221)/(\frac{1}{2}1\frac{3}{2})$

LVO bulk exhibits an $(a^- b^+ a^-)$ tilt system indicating in-phase rotations along the orthorhombic long axis b_o.[28] Furthermore, a previous study done by our group showed that LVO grown on a cubic (001)-oriented $SrTiO_3$ substrate is mainly oriented with the long axis in the plane of the substrate and underlines the presence of 90°-oriented domains rather than in-phase rotations along a_p and b_p.[39] The experimental observations made here confirm this assumption. The intensity of the $(hk0)_p$ peaks in Fig. 5 is one order of magnitude lower than that of the other two, suggesting that a negligible part of the sample exhibits an in-phase rotation along the out-of-plane direction. We make the assumption here that we do not have in-phase rotation along the pseudocubic c_p direction. The observation of the $(0kl)_p$ and $(k0l)_p$ reflections allows us to conclude that in-phase rotations occur along both two perpendicular directions within the surface plane.

In addition, we have shown that c_p is perpendicular to the substrate plane, constraining the values of the rotation angles around both in-plane pseudocubic parameters a_p and b_p to be equal. Furthermore, the relation $a_p = b_p < c_p$ allows us to assume that the tilt system of our film is $(a^- a^+ c^-)$, considering that the oxygen displacements are similar to the bulk (meaning in a rotation sense). According to Woodward, such a tilt system is associated with the maximal nonisomorphic subgroup $P2_1/m$.[21]

To further characterize the structure, it is also interesting to quantify the rotation angles. In the case of $LaVO_3$, the displacement of the La cations also contributes to the distortion of the structure. The theoretical diffraction powder patterns based on measured bulk displacement produced by the structure determined by Bordet *et al.*[28] with (1) no La displacement nor octahedral rotation, (2) La displacements but no octahedral rotation, (3) no displacement but with octahedral rotations, and (4) octahedral rotation and La displacement, are represented in Fig. 6 (all patterns were simulated for a wavelength of $\lambda = 1.0$ Å, and in the orthorhombic *Pnma* space group). By comparing the reflections produced by each contribution, it is possible to identify which peaks in the diffraction pattern are associated with the octahedral rotations and with the cation displacements (see Table I).

Experimentally, we confirm the La displacements by observing the presence of the reflection $(\frac{1}{2}\frac{1}{2}\frac{1}{2})_p$. Thus, in the calculations of the octahedral rotation we have only considered

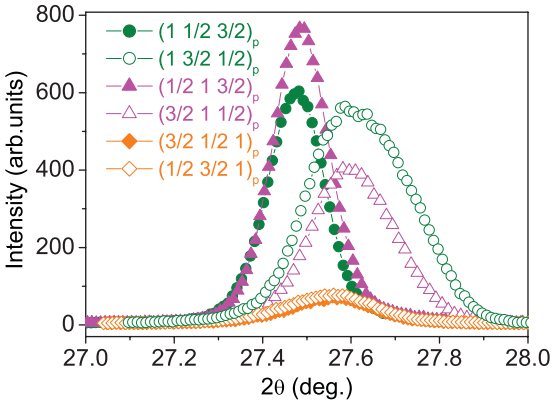

FIG. 5. (Color online) XRD patterns of the half-order peaks produced by in-phase octahedral rotations.

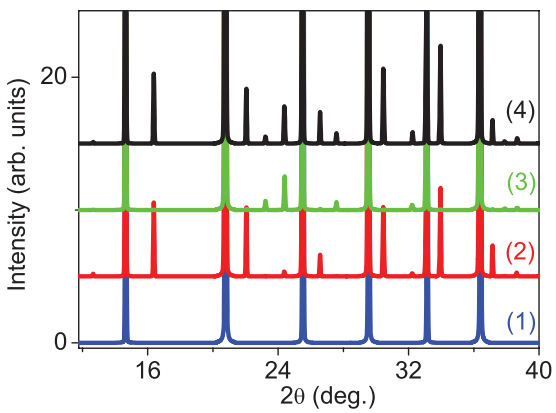

FIG. 6. (Color online) Theoretical powder diffraction patterns of $LaVO_3$ produced by the structure with: (1) neither La displacement nor octahedral rotation, (2) La displacements but no octahedral rotation, (3) no displacement but with octahedral rotations, and (4) octahedral rotation and La displacement.

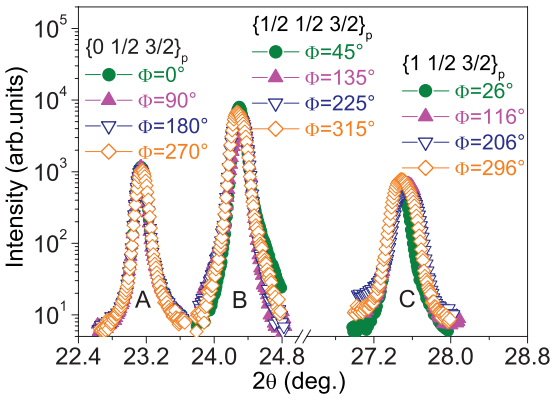

FIG. 7. (Color online) XRD patterns of equivalent half-order peaks. *A*, *B*, and *C* correspond to the peak family $\{0\frac{1}{2}\frac{3}{2}\}_p$, $\{\frac{1}{2}\frac{1}{2}\frac{3}{2}\}_p$, and $\{1\frac{1}{2}\frac{3}{2}\}_p$, respectively; see text for details.

the reflections where k is even and the two others are odd and different, since the intensity of these reflections is only generated by the octahedral rotation [reflections from the pattern (3) in Fig. 6 and Table I]. Furthermore, the rotation pattern has been determined experimentally as being (a^- a^+ c^-). Such a tilt system can produce four different structural domains. Considering the closest octahedron of the origin of the "double" unit cell, the octahedron can rotate clockwise or counterclockwise along each direction. Then, the rotations of this first octahedron force the nearest octahedra to rotate in a particular way to ensure the continuity of the lattice, and so on with the other octahedra of the cell. This produces eight combinations of clockwise/counterclockwise along the three rotational axes, which correspond to different structural domains. It turns out that these combinations give different structure factors for a specific reflection. According to our tilt system, antiphase rotations are along two directions, which reduces the number of domains by half, due to the symmetry between the domains (for example, the domain counterclockwise-clockwise-counterclockwise is the same as the domain clockwise-clockwise-clockwise). It is important to notice that the crystal symmetry is similar for all domains, since only the direction of the oxygen atoms displacement is different. The proportion of each domain can easily be determined experimentally by measuring a specific family of reflections (with a fixed l value), produced by the tilt system, which are symmetrically equivalent.[26] The resulting XRD patterns of three different families are displayed in Fig. 7. For each family, *A*, *B*, and *C*, the four peaks have the same intensity, suggesting that the four domains produced by the tilt system have equal proportions. According to those considerations, the rotation angles can be determined by the integrated intensity of the defined specific peaks using the following equation:[43]

$$I_{\mathrm{mes},i} = I_0 \frac{1-\exp\left(\frac{-2\mu T}{\sin\theta_i \cos\chi}\right)}{1-\exp\left(\frac{-2\mu T}{\sin\theta_i}\right)} \frac{1}{\sin(2\theta)} \left(\sum_{j=1}^{4} D_j |F_{hkl}|^2\right), \quad (6)$$

where I_0 is the incident photon flux, and μ and T are the linear absorption coefficient and the thickness of the film, respectively. θ is the scattering angle, χ is the tilt angle of the sample, D_j is the proportion of the structural domains produced by the rotation pattern, and F_{hkl} is the structure factor for each Bragg peak considered. Since we only consider the specific reflections produced by the octahedral rotations, the structure factor results exclusively from the oxygen atoms as expressed by the following equation:

$$F_{hkl} = f_{O^{2-}} \left(\sum_{n=1}^{24} \exp[2\pi i(hu_n + kv_n + lw_n)]\right), \quad (7)$$

where $f_{O^{2-}}$ is the O^{2-} scattering factor and the oxygen n is at the position (u_n, v_n, w_n) in the double pseudocubic unit cell.

In our calculation, we describe the system as a nonprimitive unit cell built from eight pseudocubic unit cells where the La and V cations are assumed to stay at their ideal position. That is, the La atom is at the corner and the V atom is at the body-centered positions, whereas the oxygen atoms are located at the face-centered positions.

The tilt angles of the BO_6 octahedra were then determined using the measured integrated intensity of several reflections given in Table II. The peaks are indexed in the pseudocubic cell $(hkl)_p$, as well as in the corresponding distorted orthorhombic cell $(hkl)_o$. According to the well known Glazer notation,[20] we define the rotation angles α, β, and γ as the octahedral rotation angle around the $[100]_p$, $[010]_p$, and $[001]_p$ axes, respectively (note that these angles are different from the orthorhombic structure angles α_o, β_o, and γ_o defined above). We also considered that $\alpha = \beta$ because of the strain induced by the substrate along the axis $[100]_p$ and $[010]_p$. We obtain $\alpha = \beta \simeq 3.1(1.7)^\circ$ and $\gamma \simeq 11.3(1.8)^\circ$. The associated calculated intensities were obtained by using the evaluated angles in the calculation.

According to May *et al.*,[26] the determination of the rotation angles can be used to calculate the bond angle V-O-V, and to understand the changes in the orbital interactions within the strained thin film. In their $LaNiO_3$ compound, the La and Ni cations are indeed not displaced so they can completely determine the atomic structure of $LaNiO_3$ using only the calculated tilt angles. In the case of LVO, the situation is different since we observed reflections such as $(\frac{1}{2}\frac{1}{2}\frac{1}{2})$ indicating that the La cations are displaced. Thus we cannot determine the exact atomic structure of the film yet. However, the comparison of the obtained rotation angles to the bulk ones ($\alpha \simeq \gamma \simeq 8.7^\circ$ and $\beta \simeq 7.9^\circ$, estimated from the structural

TABLE II. Relative measured and calculated peak intensities with respect to $I[(\frac{3}{2}0\frac{1}{2})_p]$, I_M, and I_C, respectively, for a film of $LaVO_3$ grown on a (001)-oriented $SrTiO_3$ substrate. $(hkl)_p$ and $(hkl)_o$ peaks are indexed both in the pseudocubic and distorted orthorhombic cell, respectively. The values of the rotation angles $\alpha = \beta \simeq 3.1(1.7)^\circ$ and $\gamma \simeq 11.3(1.8)^\circ$ were calculated based on I_M. See text for details.

Peak $(hkl)_p$	Peak $(hkl)_o$	I_M	I_C
$(\frac{3}{2}0\frac{1}{2})$	$(20\bar{1})$	1.0	1.0
$(\frac{3}{2}1\frac{1}{2})$	$(22\bar{1})$	0.671	0.673
$(\frac{\bar{1}}{2}1\frac{3}{2})$	(122)	0.202	0.188
$(\frac{1}{2}\bar{1}\frac{3}{2})$	$(2\bar{2}1)$	0.205	0.189
$(\frac{1}{2}1\frac{3}{2})$	(221)	0.154	0.189

data given by Bordet *et al.*[28]) shows that the rotation around the $[001]_p$ axis is enhanced due to the reduced lattice parameter as a result of the bidimensional compressive stress, while the rotations around the $[100]_p$ and $[010]_p$ axis are reduced due to the degree of freedom along the $[001]_p$ direction. Furthermore, the knowledge of the rotation angles allows us to evaluate the V-O-V bond angle in our system to be 156.6(4.4)° along the a_p and b_p directions and 171.3(4.8)° along the c_p direction, while in bulk these angles are 158.8° along the a_p and c_p directions and 155.4° along the b_p direction. This difference reveals that substrate-induced biaxial stress plays an important role in the orbital overlapping in thin films. Such a quantitative methodology to determined V-O-V angles in the case of $LaVO_3$ thin film could be applied to many other strained perovskite compounds having a *Pnma* space group.[7,25]

IV. CONCLUSIONS

In conclusion, we have demonstrated that $LaVO_3$ under compressive stress adopts a distorted orthorhombic structure in which the octahedra rotate to accommodate the substrate-induced strain. Surprisingly, the magnitudes of the tilt angles change from the bulk values. Using the measured intensity of specific diffraction reflections exclusively produced by the oxygen displacements, we have been able to evaluate the tilt angles to be 3.1(1.7)° around the $[100]_p$ and $[010]_p$ axes, and 11.3(1.8)° around the $[001]_p$ axis. The next step would be to control the magnitude of the rotation angles using different substrates[26] or by stacking two materials together in a repetitive way where one constrains the other all along the thickness of the superlattice.[44] Such a study could help to interpret the observed modification in physical properties of systems such as $LaVO_3/SrVO_3$ superlattices[34,38] or even enable us to simulate the band structure of more complex systems.

ACKNOWLEDGMENTS

This research was partly supported by the ANR GeCoDo project. The authors would like to acknowledge the scientific insights and a careful reading of the article by Steven J. May at the Department of Materials Science and Engineering, Drexel University. H.R. and W.P. would also like thank B. Mercey, O. Perez, P. Boullay, and V. Duffort for their continuous encouragement during this work.

*helene.rotella@ensicaen.fr
†wilfrid.prellier@ensicaen.fr

[1] G. Smolenskii and V. Bokov, J. Appl. Phys. **35**, 915 (1964).
[2] J. Wang, J. B. Neaton, H. Zheng, V. Nagarajan, S. B. Ogale, B. Liu, D. Viehland, V. Vaithyanathan, D. G. Schlom, U. V. Waghmare *et al.*, Science **299**, 1719 (2003).
[3] D. Dijkkamp, T. Venkatesan, X. D. Wu, S. A. Shaheen, N. Jisrawi, Y. H. Min-Lee, W. L. McLean, and M. Croft, Appl. Phys. Lett. **51**, 619 (1987).
[4] J. Hamet, B. Mercey, M. Hervieu, and B. Raveau, Physica C **193**, 465 (1992).
[5] A. David, P. Boullay, R. V. K. Mangalam, N. Barrier, and W. Prellier, Appl. Phys. Lett. **96**, 221904 (2010).
[6] J. He, A. Borisevich, S. V. Kalinin, S. J. Pennycook, and S. T. Pantelides, Phys. Rev. Lett. **105**, 227203 (2010).
[7] H. Y. Hwang, T. T. M. Palstra, S.-W. Cheong, and B. Batlogg, Phys. Rev. B **52**, 15046 (1995).
[8] J. Goodenough, Rep. Prog. Phys. **67**, 1915 (2004).
[9] R. Søndenå, S. Stølen, P. Ravindran, T. Grande, and N. L. Allan, Phys. Rev. B **75**, 184105 (2007).
[10] P.-E. Janolin, B. Dkhil, P. Bouvier, J. Kreisel, and P. Thomas, Phys. Rev. B **94**, 094218 (2006).
[11] P.-E. Janolin, P. Bouvier, J. Kreisel, P. A. Thomas, I. A. Kornev, L. Bellaiche, W. Crichton, M. Hanfland, and B. Dkhil, Phys. Rev. Lett. **101**, 237601 (2008).
[12] G. Samara, T. Sakudo, and K. Yoshimitsu, Phys. Rev. Lett. **35**, 1767 (1975).
[13] P. Bouvier and J. Kreisel, J. Phys.: Condens. Matter **14**, 3981 (2002).
[14] R. Angel, J. Zhao, and N. Ross, Phys. Rev. Lett. **95**, 025503 (2005).
[15] T. Tohei, A. Kuwabara, T. Yamamoto, F. Oba, and I. Tanaka, Phys. Rev. Lett. **94**, 035502 (2005).
[16] J. Zhao, N. L. Ross, and R. J. Angel, Acta Crystallogr. Sect. B **60**, 263 (2004).
[17] J. Zhao, N. L. Ross, and R. J. Angel, Acta Crystallogr. Sect. B **62**, 431 (2006).
[18] M. Guennou, P. Bouvier, B. Krikler, J. Kreisel, R. Haumont, and G. Garbarino, Phys. Rev. B **82**, 134101 (2010).
[19] A. Glazer, Acta Crystallogr. Sect. B **28**, 3384 (1972).
[20] A. Glazer, Acta Crystallogr. Sect. A **31**, 756 (1975).
[21] P. Woodward, Acta Crystallogr. Sect. B **53**, 32 (1997).
[22] P. Woodward, Acta Crystallogr. Sect. B **53**, 44 (1997).
[23] S. Bhattacharjee, E. Bousquet, and P. Ghosez, Phys. Rev. Lett. **102**, 117602 (2009).
[24] E. Bousquet and N. Spaldin, Phys. Rev. Lett. **107**, 197603 (2011).
[25] T. Günter, E. Bousquet, A. David, P. Boullay, P. Ghosez, W. Prellier, and M. Fiebig (unpublished).
[26] S. J. May, J.-W. Kim, J. M. Rondinelli, E. Karapetrova, N. A. Spaldin, A. Bhattacharya, and P. J. Ryan, Phys. Rev. B **82**, 014110 (2010).
[27] A. Vailionis, H. Boschker, W. Siemons, E. P. Houwman, D. H. A. Blank, G. Rijnders, and G. Koster, Phys. Rev. B **83**, 064101 (2011).
[28] P. Bordet, C. Chaillout, M. Marezio, Q. Huang, A. Santoro, S.-W. Cheong, H. Takagi, C. S. Oglesby, and B. Batlogg, J. Solid State Chem. **106**, 253 (1993).
[29] M. Lufaso and P. Woodward, Acta Crystallogr. Sect. B **57**, 725 (2001).
[30] J.-S. Zhou and J. B. Goodenough, Phys. Rev. Lett. **94**, 065501 (2005).
[31] M. Reehuis, C. Ulrich, K. Prokeš, S. Mataš, J. Fujioka, S. Miyasaka, Y. Tokura, and B. Keimer, Phys. Rev. B **83**, 064404 (2011).
[32] J. Fujioka, T. Yasue, S. Miyasaka, Y. Yamasaki, T. Arima, H. Sagayama, T. Inami, K. Ishii, and Y. Tokura, Phys. Rev. B **82**, 144425 (2010).

[33]U. Lüders, W. C. Sheets, A. David, W. Prellier, and R. Frésard, Phys. Rev. B **80**, 241102 (2009).
[34]A. David, R. Frésard, P. Boullay, W. Prellier, U. Lüders, and P.-E. Janolin, Appl. Phys. Lett. **98**, 212106 (2011).
[35]S. Miyasaka, T. Okuda, and Y. Tokura, Phys. Rev. Lett. **85**, 5388 (2000).
[36]A. Fouchet, W. Prellier, B. Mercey, L. Méchin, V. N. Kulkarni, and T. Venkatesan, J. Appl. Phys. **96**, 3228 (2004).
[37]Y. Hotta, H. Wadati, A. Fujimori, T. Susaki, and H. Y. Hwang, Appl. Phys. Lett. **89**, 251916 (2006).
[38]W. Sheets, P. Boullay, U. Lüders, B. Mercey, and W. Prellier, Thin Solid Films **517**, 5130 (2009).
[39]P. Boullay, A. David, W. C. Sheets, U. Lüders, W. Prellier, H. Tan, J. Verbeeck, G. V. Tendeloo, C. Gatel, G. Vincze *et al*., Phys. Rev. B **83**, 125403 (2011).
[40]URL http://www.public.asu.edu/∼mtreacy/DIFFaX.html.
[41]R. Khan and M. Akhtar, Solid State Commun. **137**, 110 (2006).
[42]L. Lutterotti, D. Chateigner, S. Ferrari, and J. Ricote, Thin Solid Films **450**, 34 (2004).
[43]D. Chateigner, *Combined Analysis* (ISTE, London & Wiley, New Jersey, 2010).
[44]S. J. May, C. R. Smith, J.-W. Kim, E. Karapetrova, A. Bhattacharya, and P. J. Ryan, Phys. Rev. B **83**, 153411 (2011).